International Geotechnical Symposium on Theory and Practice of Earth Reinforcement / Fukuoka Japan / 5-7 October 1988

Experimental studies on the performance of polymer grid reinforced embankment

H.Miki & K.Kutara
Public Works Research Institute, Ministry of Construction, Ibaragi, Japan
T.Minami
Tokyu Construction Co., Ltd, Tokyo, Japan
J.Nishimura
Mitsui Petrochemical Industries Ltd, Tokyo, Japan
N.Fukuda
Fukken Co., Ltd, Yokohama, Japan

ABSTRACT: In order to establish an appropriate design and execution method for reinforcing the earth embankment with polymer grids (hereinafter grids) a series of experiments and analyses were conducted by constructing large-size test embankments. The dimensions of the experimental enbankment were: - height : 3 m, slope : 1:0.7, the length and spacing of grid laying in the embankment were varied and the reinforcing effects, when tested under a severe condition of 15 mm/hr artificial rain, were compared and evaluated. The integration effect of grid and earth was determined quantitatively through the analyses of slip-circle method and elasto-plastic FEM. The applicablity of FEM to the grid reinforced embankment analysis was discussed.

1 INTRODUCTION

The advantages of using the grids as reinforcements are various. The possibility of constructing steep embankments due to grid reinforcement enable us to effectively utilize the available construction space, which is one important factor in land scarce Japan, thus reducing the quantity of fill-material especially in road-construction works in mountainous areas. As a result of grid reinforcement, the embankment has got a resistance to torrential rain or earthquake. Morever, using the vegetative cover it was made possible to beautify the slope of embankment.

At present the design of grid-reinforced embankment is based for convenience on the concept of applying the tensile strength of reinforcing material to the slip-circle failure analysis (see Miki et al. (1986) and Kutara et al. (1987)). Doubtless it could not necessarily explain the true nature of the mechanism of reinforcement.

Thus the present research is undertaken with a view to formulate a rational method of design and construction of grid reinforced embankment in corporating the mechanism of reinforcement with due consideration of the effect of grid laying pattern under a heavy rain.

Table 1 Test cases.

Test case	Grid laying length L	Grid laying layer N
Case 0.0	0	0
Case 1.3	1	3
Case 2.3	2	3
Case 3.3	3	3
Case 3.1	3	1
Case 3.2	3	2
Case 3.3	3	3

2 PROCEDURE

2.1 Instrumentation and test conditions

The representative test embankments and salient features of reinforcement are as shown in Fig. 1 and Table 1. Three cases of grid laying length - 1 m, 2 m and 3 m and three cases of grid layers - 1-layer, 2-layer and 3-layer were investigated. The combination of grid laying length and grid layer is as shown in Table 1. Here the measurement of embankment's inner and surface deformations were conducted by using displacement gauges and inclinometers respectively. The strains on polymer grids were measured by foil strain gauges attached to grids. Ground water depths were measured by manometers inserted in the embankment. The moisture distribution inside the embankment were measured by radio-isotopes to determine the degree of saturation. The settings of those instruments were as shown in Fig. 1 and Fig. 2.

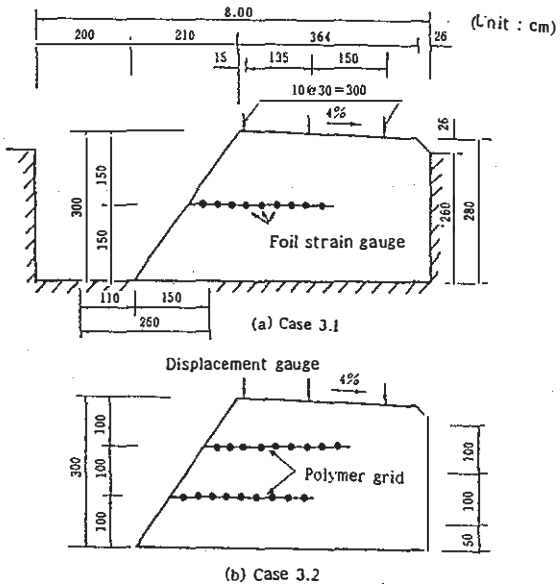

Fig. 1 Standard sections of reinforced embankment.

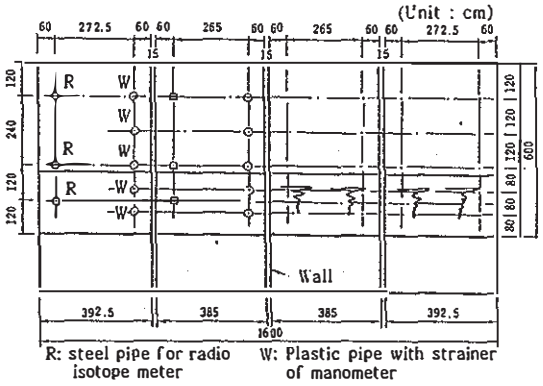

Fig. 2 Plan of test embankment.

2.2 Characteristics of fill-material and polymer grid

The choice of fill-material was done under the condition that the slope safety factor was greater than 1.0 during construction and less than 1.0 under heavy rain. Thus the mountain sand distributed in Ibaraki Prefecture was used as a fill-material for the embankment as it satisfied the above condition (see Table 2). The dry density of compacted soil at a degree of 80% compaction is 1.41 t/m^3 (average). The moisture content is 22% and degree of saturation is 70%. The shear strength of the soil under the above conditions is c_u=0.7 tf/m^2 and angle of internal friction ϕ_u=20.1°.

The bi-axial stretched polymer grids (SS-2) were used and their properties are : -weight : 320 gf/m^2, strength : 1.8 tf/m, peak strain: 8% in longitudinal direction.

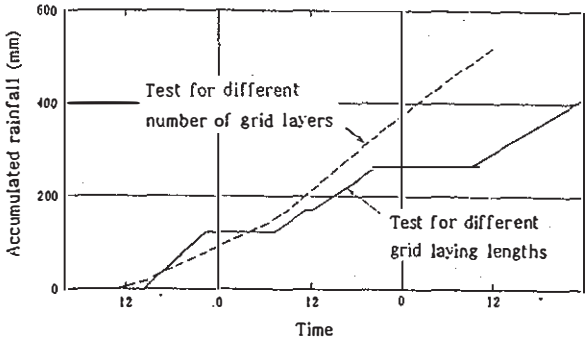

Fig. 3 Relationship between accumulated rainfall and elapsed time.

Table 2 Salient features of fill-material.

Natural water content	ωn(%)	22.4-24.3
Specific gravity	Gs	2.70
Gravel fraction	(%)	1-2
Sand fraction	(%)	70-74
Silt fraction	(%)	12-20
Clay fraction	(%)	9-12
Maximum grain size	(mm)	4.76
Uniformity coefficient	Uc	5.5-15.9
Compaction test method	(by JIS)	1.6.b
Optimum moisture content	ωopt(%)	17.0-18.6
Maximum dry density	ρdmax(t/m^3)	1.64-1.70
Permeability	k(cm/s)	$1.5-1.6\times10^{-4}$

3 TEST RESULTS

3.1 Test results for different grid laying lengths

The tests were conducted by constructing four cases of embankment-one case without reinforcement (Case 0.0), 3 cases of grid laying length 1m, 2m, 3m each having 3-layers of grids: Case 1.3, Case 2.3 and Case 3.3. The relationship between accumulated rainfall and the development pattern of deformation for each case are as shown in Fig. 3. When viewed from the accumulated rainfall, the failure of slope surface took place at 145 mm for Case 0.0 and when the accumulated rainfall reached 235 mm the sliding (collapse) occurred along the plane outside the reinforced zone in the Case 1.3; and also in the case of Case 2.3 only cracks occurred along the inner edge of the reinforced zone, but in the case of Case 3.3 the embankment was stable without any cracks even at the accumulated rainfall 450 mm but it was with only a minor erosion and settlement of several centimeters. The distribution of saturation degree of fill-material, distribution of grids strain and settlement of embankment surface are as shown in Fig. 4. These values are measured during the 15mm/hr artificial rain.

At the time of slope failure (collapse)

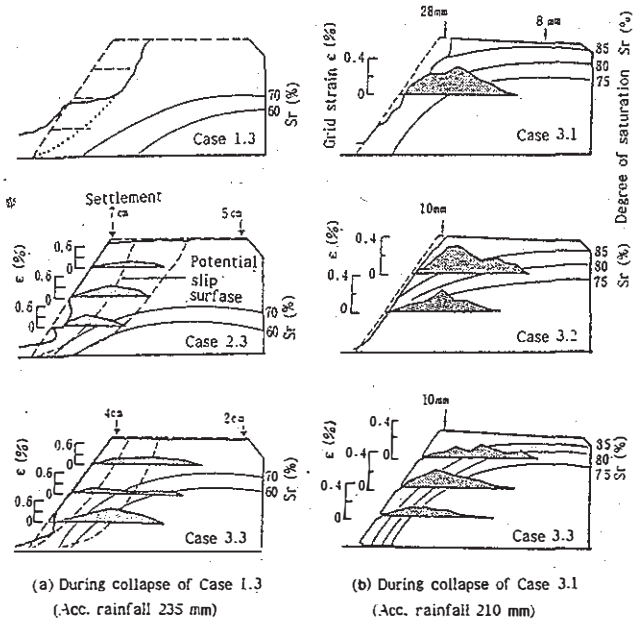

(a) During collapse of Case 1.3 (Acc. rainfall 235 mm)

(b) During collapse of Case 3.1 (Acc. rainfall 210 mm)

Fig. 4 Relationship between embankment deformation, grid strain distribution and saturation degree.

of Case 0.0, the peak strain εmax of Case 1.3 occurred at the inner side near estimated sliding plane of the embankment (Refer to Fig. 4). Similarly, in Case 2.3 and Case 3.3 the εmax occurred at the same position of the sliding plane estimated in Case 1.3.

At the time of slope failure (collapse) of Case 1.3 the range of εmax of Case 2.3 and Case 3.3 are increased to 0.16 - 0.33% and 0.22 - 0.41% respectively.

3.2 Test results for different number of grid layers

In this testing of embankment, the grids are laid horizontally with a length of 3m and three kinds of layers: 1-layer, 2-layer and 3-layer which are called Case 3.1, Case 3.2 and Case 3.3 respectively. The embankment deformations and the accumulated artificial rainfall are shown in Fig. 3. The embankment deformations, grid-strain distribution and the distribution pattern of saturation at the time of accumulated rainfalls 210 mm and 540 mm are as shown in Fig. 4.

When the accumulated rainfall reached 110 mm in the Case of Case 3.1, the deformation (horizontal displacement) of the top of slope increased rapidly and at the time of 210 mm rainfall, the slope was eroded for a depth of 50 cm. In the case of Case 3.2 and Case 3.3 there was only a surface erosion without any sliding until the accumulated rainfall

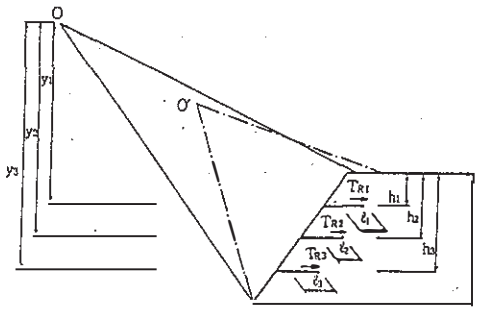

Fig. 5 Embankment section used in stability analysis.

reached 540 mm i.e the final rainfall of the test. At the initial stage of the test, the saturation degree of the inner fill was 65% to 70%. It increased gradually starting from the outer surface with the increase of accumulated rainfall. The sliding (collapse) area of the embankment of Case 3.1 was found to have a saturation degree of over 85%. As to the grid strain, it was less than 0.4% in all cases, which means that the grid strain was not considerably high during the rainfall test.

4 ANALYSIS OF REINFORCING EFFECT BY SLIP-CIRCLE METHOD

4.1 Basic equation for evaluating the internal stability of reinforced embankment

The basic equation that has been used for the usual practice of reinforced embankment design is:

$$Fs = \frac{Mr + \Delta Mr}{Md} = \frac{Mr + \Sigma(Tri \times yi)}{Md} \quad .....(1)$$

Refer to Fig. 5

Here Mr: the resisting moment of soil mass
Md: the driving moment of soil mass
ΔMr: the resisting moment due to grid reinforcements
Tri: pull-out resisting force due to ith layer of grid reinforcement
yi: the vertical distance of the ith layer of grid to the center of the slip-circle

This equation is meant for checking the internal stability of the reinforced zone of the embankment. Tri is determined by the smaller value of either the allowable tensile strength Ta (0.75 tf/m) of grid or the pull-out grid resistance Tpi which is given by the equation (2).

$$Tpi = 2.\sigma i.\tan\phi.li \quad .....(2)$$

Here σi = the vertical stress on the ith layer grid

li = the bonding length of ith layer grid

The constant 2 means that the frictional resestance is acting on both sides of grid.

4.2 An equation concerning the integration effect or increased apparent cohesion

The safety factor Fs* which is obtained by substituting the value of Tri in equation (1) with the tension T derived by multiplying grid strain εi with stiffness J (73 tf/m) is found to be smaller than the Fs obtained by the equation (1) with pull-out resistance force Tri. It is to be concluded that this is due to the fact that the grid and earth are integrated into a rigid body with a decreased deformation on account of the grid reinforcement. This integration effect will be quantitatively studied by conducting tests on embankments with different layered grids.

Here it is considered that the greater the difference of Fs and Fs* (ΔFs) is, the higher the integration effect will be. The increase of an apparent cohesion (Δc) which results in the ΔFs can be computed by the back-analysis using the equation (3).

$$\Delta Fs = Fs - Fs^* = \frac{R\ \Delta c\ \Sigma 1}{Md} \qquad .....(3)$$

where R: the radius of slip-circle

$\Sigma 1$; the length of slip-circle arc.

And also the rate of increase of apparent cohesion (Rc) can be determined by the following equation:

$$Rc = \frac{c + \Delta c}{c} \qquad .....(4)$$

In that the increase of apparent shear strength due to laying of grids is considered as the increase of cohesion combined altogether.

4.3 Result of analysis

The analyses were done under the following conditions.

(a) At the time of rainfall (acc. rainfall 150 mm) when the sliding (collapse) of embankment took place in the case without reinforcement (Case 0.0).

(b) At the time of rainfall (acc. rainfall 265 mm) when the sliding (collapse) occurred in the case with 1-m long reinforcement (Case 1.3).

The strength parameters of the embankment (c,ϕ) can be checked by means of back-analysis for the Case 0.0 without reinforcement. In that the unit weight of the fill material will be increased from 1.70 to 1.85 tf/m^3 and the internal angle of friction is assumed to be 20°; that is taken constant throughout the testing and the cohesion only decreases with the increase of degree of saturation.

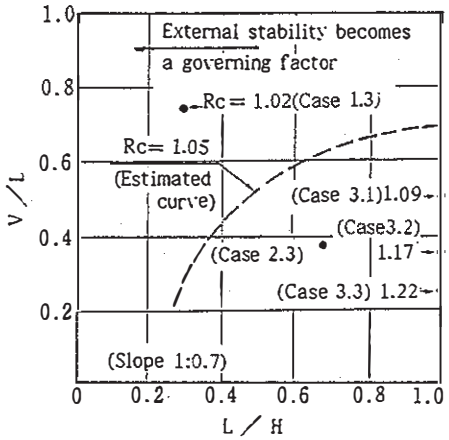

Fig. 6 Relationship between V/L, L/H and Rc.

Table 3 Analysis for the integration effect at collapse without reinforcement.

Test case	The drive moment Md (tf.m)	The resisting moment Mr (tf.m)	Arc length yi (m)	Measured strain εm x10^{-6}	The resisting moment due to grid ΔMr (tf/m)		Pullout resistance Tp (tf/m)	Allowable tensile strength Ta (tf/m)	Fs* based on measured strain	Fs by eq. (1)	Apparent cohesion C+ΔC (tf/m^2)	Rc $\frac{C+\Delta C}{C}$
3.1	15.48	13.48	5.00	9670	1.19		0.269	0.75	1.08	1.09	0.367	1.09
3.2			4.50	2600	0.85	1.17	0.364					
			5.50	800	0.32		0.236		1.08	1.19	0.393	1.17
3.3			4.25	1000	0.31		0.283					
			4.25	1600	0.58	1.23	0.323		1.08	1.23	0.410	1.22
			5.75	800	0.34		0.135					
2.3	14.23	14.23	4.25	1800	0.56		0.269					
			5.00	2000	0.73	2.13	0.292		1.15	1.24	0.346	1.02
			5.75	2000	0.84		0.136					

On the basis of the above conditions for Case 0.0 the cohesion is computed to be 0.337 tf/m^2. From the results of measurement of grid strains for the reinforced embankment the increase of apparent cohesion can be determined by using equation (3). And the rate of increase of apparent cohesion can be computed by equation (4).

Table 3 describes the results of computation for Fs*, Fs and Rc for different cases of reinforcement. Fig. 6 describes the relationship between the grid laying pattern and the rate of increase of apparent cohesion (Rc). In that the grid laying pattern is represented by the vertical spacing divided by grid laying length (V/L) and laying length divided by embankment height (L/H). From this graph it is learnt that the smaller V/L and the bigger L/H is the higher the value of Rc will be. That is to be considered that the integration effect is vividly increased.

5 NUMERICAL ANALYSIS BY FEM

5.1 Analysis model

The analysis model is as shown in Fig. 7. That is the elasto - plastic model of finite element method. Embankment fill-material is considered as a complete elasto-plastic body by Drucker-Prager's constitutive equation. And grids are considered as elasto-plastic spring element. The analysis conditions are the same as those described in section 4.3.

The increase of unit weight and the decrease of shear strength (cohesion) due to increased saturation are considered in the analysis. The parameters of the material are as shown in Table 4. The analyses are done for the different cases as stated in Table 1.

Table 4 Properties of materials.

Earth fill (Drucker-Prager model)	Unit weigth (natural)	γ_t	(tf/m^3)	1.70
	Unit weight (saturated)	γ_{sat}	(tf/m^3)	1.85
	Elastic modulas	E	(tf/m^2)	30.0
	E after yield	E'	(tf/m^2)	0.0
	Cohesion (natural)	c	(tf/m^2)	0.7
	Cohesion (saturated)	c	(tf/m^2)	0.0175(*)
	Angle of internal friction		(o)	20.0
	Poisson's ratio			0.30
Polymer grid (Spring model)	Spring modulas	AE	(tf)	50.0
	AE after yield	AE'	(tf)	0.0
	Tensile strength	T	(tf/m)	1.8

(*) Determined by backanalysis at the collapse without reinforcement (Case 0.0, acc. rainfall : 150 mm)

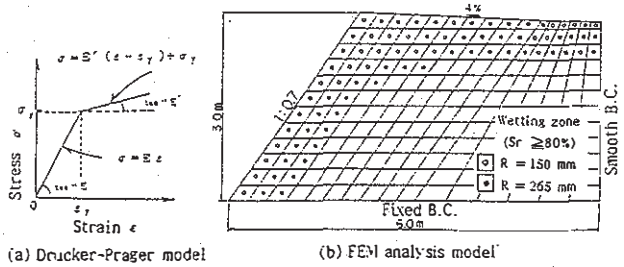

(a) Drucker-Prager model (b) FEM analysis model

Fig. 7 Outline of analysis model.

5.2 Results of analysis

The horizontal displacement of embankment slope and the grid-strain distribution are as shown in Fig. 8. The comparison of reinforcing effects for the different number of grid layers can be seen in Fig. 8 (a) to (c). At the initial time of rainfall testing the difference of reinforcing effects is not clearly defined. But after the rainfall when the sliding (collapse) of the embankment without reinforcement occurs, the embankment deformation has turned out to be smaller with the increased number of grid layers. As to the grid strains, the results of the tests were found to be in close conformity with those obtained by FEM analyses. When the saturation get deeper inside the embankment, the peak strain on grid is found at a place nearer to the slope.
Thus this result in the increase of fill-material's unit weight and the decrease of cohesion at a comparatively high rate along the saturation line.

The local safety factor and the embankment deformations for Case 3.3 are changed with the increase of accumulated rainfalls. These results are shown in Fig. 9. These results are actually the standard results that are obtained from the analyses for different cases. And this analysis method explains sufficiently the reinforcing mechanism in the embankment.

6 CONCLUSION

In this report the large-size grid reinforced embankments were constructed and testings with analyses were done especially with artifical rainfalls and the effect of reinforcement is studied for the embankments with different layers of grids. The results of testing can be concluded as follows: -

(1) In the testings with the grids laying 0.75 m vertically spaced, for the Case 1.3 with the rates of laying length

to embankment height (L/H) ≤ 0.33 the external stability becomes a governing factor and for the case of L/H > 0.67 (Case 2.3), it is the internal stability that governs the overall stability of the embankment.

(2) When the grids are laid horizontally in several layers the deformation of the reinforced zone is so much decreased as a result of interaction between the grids and fill-material. Consequently the grids strain are considerably small i.e less than 0.4%. Thus it can be concluded that the reinforcing mechanism and its effect are quantitatively evaluated.

(3) As a quantitative estimate of integration effect of grid and fill-material the rate of increase of apparent cohesion Rc is defined and the relationship between Rc and grid laying pattern is analysed. As a result of it the smaller the value of V/L is, the bigger L/H and Rc will be. It means that the integration effect is quantitatively estimated.

(4) The FEM analysis is conducted assuming the embankment as an elasto-plastic body and the results are compared with those of the tests. The results are found to be in close conformity with each other. This means that this analysis method explains sufficiently the reinforcing mechanism in the embankment.

In addition to the present research, the testing of a practical size grid reinforced embankment (height. 6 m, slope 1:1.2) is in progress. And the authors hope that further important facts on reinforcing mechanism and construction method will be clarified in the near future.

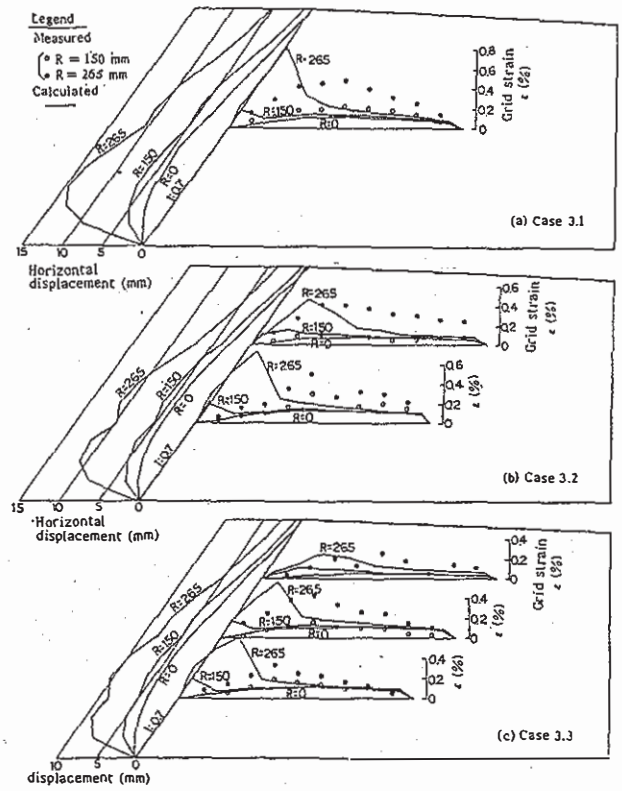

Fig. 8 Grid strain distribution and slope deformation.

REFERENCES

Miki,H. et al. 1986. Large scale experiments on the behavior of embankment reinforced with polymer grids. Proc. 1st Geotextile Symp., J.P.IGS, pp. 77-82. (in Japanese)

Kutara,k. et al. 1987. A numerical analysis of earth embankment reinforced by polymer grids. Proc. 2nd Geotextile Symp., J.P.IGS, pp.42-48. (in Japanese)

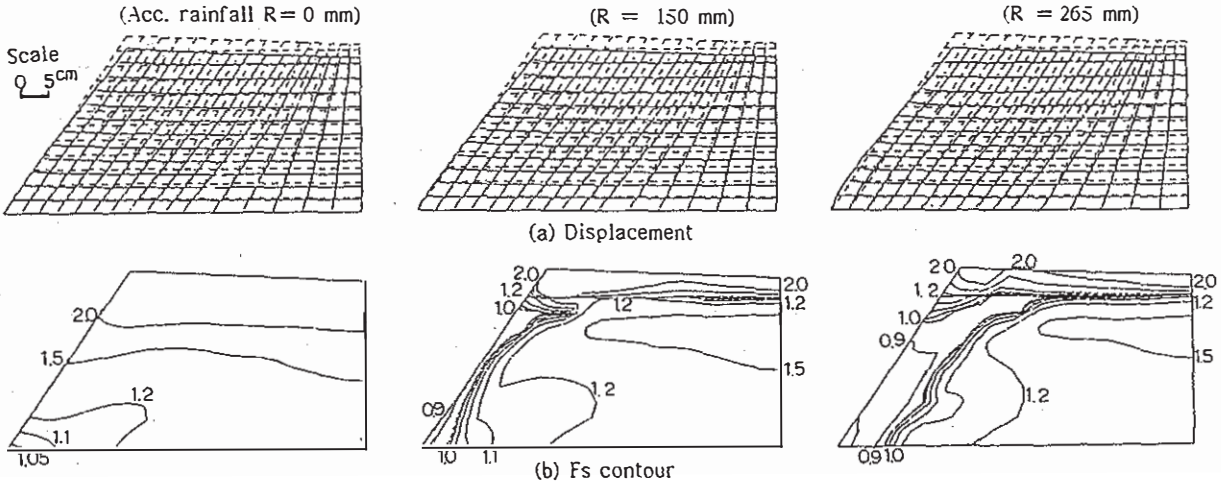

Fig. 9 Changes of deformation pattern and contour of localized safety factor(Case 3.3).